

Supplemental Information

Supplemental Figure 1. Clinicopathologic correlation of STING expression in

HNSCC patients (A) The relationship between STING IHC scores and patient age in 264 HNSCC samples was assessed using a linear regression model. The portions shaded in blue depict 95% confidence interval, the blue dashed curves represent 95% prediction interval, and the solid blue lines show the linear regression fit line. (B) After stratifying 264 HNSCC patients by HPV status, Kaplan-Meier curves were assessed based on the tertiles of HNSCC-specific STING IHC scores and a log-rank test (* $p < 0.05$).

Supplemental Figure 2. BLAST result comparing homology of HPV16 E7 and

HPV18 E7 proteins. The amino acid sequences of HPV16 E7 and HPV18 E7 were compared using the protein BLAST tool of the NCBI database. Identical amino acid sequences between these two proteins are highlighted in red.

Supplemental Figure 3. cGAMP-induced IFN-I activation is inhibited in HPV⁺

HNSCC cells. HPV⁺ UMSCC47 (A), HPV⁺ 93VU147T (B), and HPV⁻ UMSCC49 (C) cells were transfected with 5 $\mu\text{g/ml}$ cGAMP and incubated for 16h. qPCR was utilized to quantify the RNA expression levels of *IFNB1* and *CXCL9*. Comparisons between two groups were made by using two-tailed unpaired t-test (** $p < 0.01$, *** $p < 0.001$).

Results represent three independent experiments.

Supplemental Figure 4. HPV16 E7 inhibits poly(dA:dT)-induced IFN-I activation.

93VU147T (A) and UMSCC47 (B) cells were transfected with 1.0 µg/ml poly(dA:dT), in the presence or absence of 1.5 µg/ml HPV16 E7 plasmid for 24h. The mRNA levels of *IFNB1*, *CXCL10* and *ISG54* were determined by qPCR. The comparisons between two independent sets were analyzed using two-tailed unpaired t-test. (* $p < 0.05$, ** $p < 0.01$, *** $p < 0.001$, and **** $p < 0.0001$). Experiments were repeated three times.

Supplemental Figure 5. HPV16 E7 or NLRX1 has a modest effect on the

transcription levels of *STING*. (A) 93VU147T, UMSCC47, and FaDu cells were transfected with 1.5 µg/ml HPV16 E7 plasmid and incubated for 24h. The mRNA levels of *STING* were detected by qPCR. Experiments were repeated twice. (B) EV and NLRX1-deficient 93VU147T and SCC90 cells were transfected with 1.0 µg/ml *STING* plasmid for 24h, and SCC47 EV/sh-NLRX1 cells were transfected with EV plasmid alone for 24h prior to the harvest. The mRNA levels of *STING* were determined by qPCR. Experiments were repeated twice.

Supplemental Figure 6. *Il10* is decreased in shNLRX1 tumors compared with

EV tumors. Total mRNA was extracted from EV and shNLRX1 tumors and then subjected to qPCR quantitation of the expression levels of *Il10*. Values represent

mean \pm SEM of 16 control and 9 shNLRX1 tumors, which were pooled from two repeat experiments. Comparisons between two groups were made by using two-tailed unpaired t-test.

Supplemental Figure 7. The shNLRX1 tumors are more CD8⁺ T-cell-inflamed than empty vector control tumors. C57BL/6 mice were implanted with one million empty vector control or NLRX1-deficient MOC2-E6/E7 cells on right flanks and monitored for 34 days before harvest of tumors (n=8 in each group). H.&E. and CD8 IHC staining were performed (Magnification: 200 \times and 400 \times). Representative H.&E. (A) and CD8 IHC (B) sections from three representative pairs are shown.

Supplemental Figure 8. Confirmation of CD8⁺ T-cell depletion in vivo. C57BL/6 hosts were administered with 0.5mg of anti-CD8 i.p. daily injections for three days or the same volume of PBS as mock prior to tumor implantation; and then twice per week for two weeks (n=7 each group). Peripheral blood was collected on day 0 and day 4 and peripheral blood mononuclear cells were stained for CD8⁺ T-cells. (A) Gating strategy for CD8⁺ T-cells is shown. (B) Representative flow cytometric analysis of CD8⁺ T cells on day 0 and day 4 (post three doses of anti-CD8 administration) is shown.

Supplemental Figure 9. Spearman correlation analysis between gene expression levels and TIL subsets in HPV⁻ HNSCC specimens. FARDEEP was utilized to determine the frequency of major TIL subsets, including CD8⁺ T-cells, Tmem, Tregs, $\gamma\delta$ T-cells, activated NK cells, and M1-like macrophages in 420 HPV⁻ HNSCC specimens in the TCGA database. A Spearman correlation analysis was conducted to evaluate the association between the expression levels of *NLRX1* or *STING* and the frequencies of TIL subsets, with *p*-values and Spearman correlation coefficients indicated in each panel (**p*<0.05; ***p*<0.01, ****p*<0.0001). Each dot represents one HPV⁻ HNSCC specimen.

Supplemental Table 1. Demographic Information of Human HNSCC Tissue

Microarray Samples with STING Scoring Available (n=264). A total of 297 patients with primary HNSCC were recruited to the study. The tumors were reviewed by an oral and maxillofacial pathologist who circled tumor parenchyma. Tissue microarrays were generated including 3 cores per tumor specimen. At the time of the analysis, the median follow-up of these patients was 60.1 months. The cores that did not have enough tumor tissue were excluded from analysis, and STING staining scores for 264 patients were available. Their demographic information is summarized in this table.

	Category	Sample size (%)
Age	<60	146 (55%)
	60-80	106 (40%)
	>80	12 (5%)
Gender	Male	188 (73%)
	Female	71 (27%)
Stage	Stage 0/1	27 (10%)
	Stage 2	29 (11%)
	Stage 3	40 (15%)
	Stage 4	164 (63%)
HPV Status	Positive	83 (32%)
	Negative	155 (60%)
	Unknown	22 (8%)
Smoking Status	Current	117 (45%)
	Former (quit >12 months)	82 (32%)
	Never	61 (23%)
Alcohol Use	Current	172 (66%)
	Former (quit >12 months)	61 (23%)
	Never	27 (10%)
Disease Site	Oral Cavity	116 (45%)
	Oropharynx	81 (31%)
	Larynx	42 (16%)
	Hypopharynx/Other	21 (8%)

Supplemental Table 2. The hazard ratios of STING protein expression in

HNSCC cells or TME after patient stratification using HPV status Patients

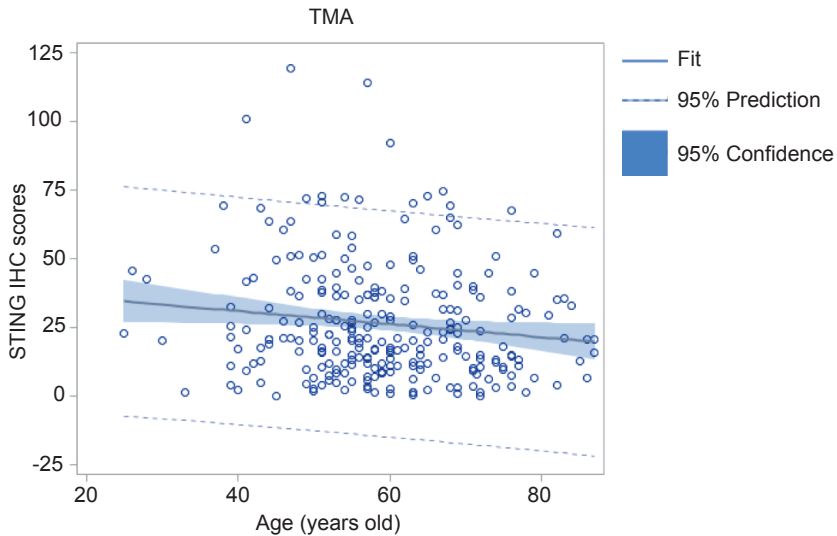
included in the TMA, as shown in Table 1 and Supplemental Table 1, were stratified by their HPV status. A multivariate Cox model controlling for age, clinical stage, disease site, comorbidities, and smoking was also used for survival comparisons.

The Hazard Ratios for the effect of tumor-specific and TME-specific STING expression levels are shown.

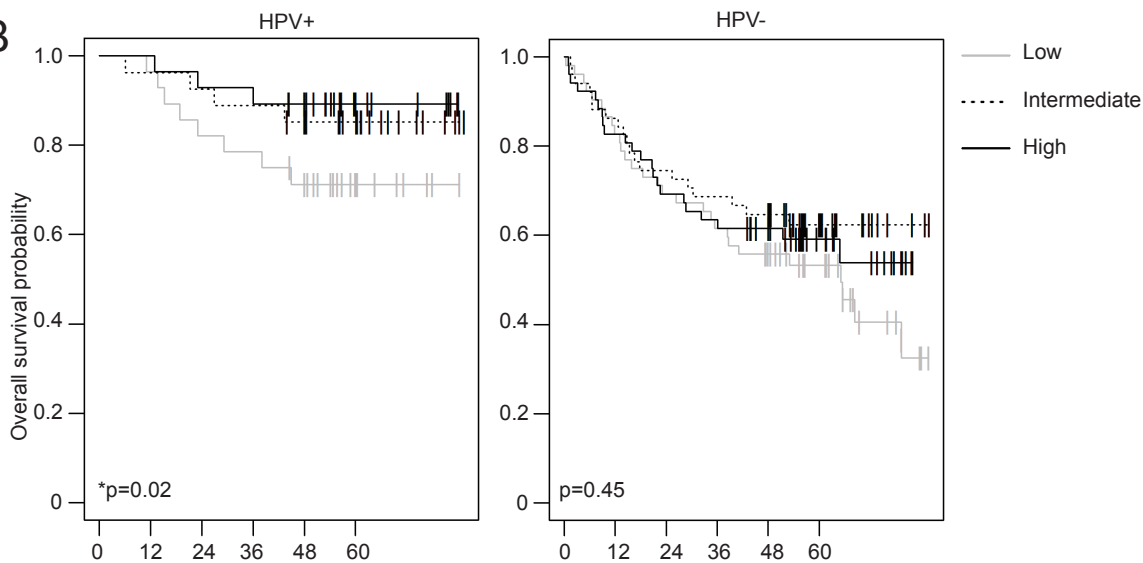
Variable	HPV+		HPV-	
	HR(95%CI)	<i>p</i> -value	HR(95%CI)	<i>p</i> -value
STING IHC Scores				
Tumor-Specific	0.95(0.91,0.99)	0.02	1.00(0.98,1.01)	0.45
TME-Specific	0.94(0.90,0.99)	0.03	1.00 (0.98,1.01)	0.68

Supplemental Figure 1

A



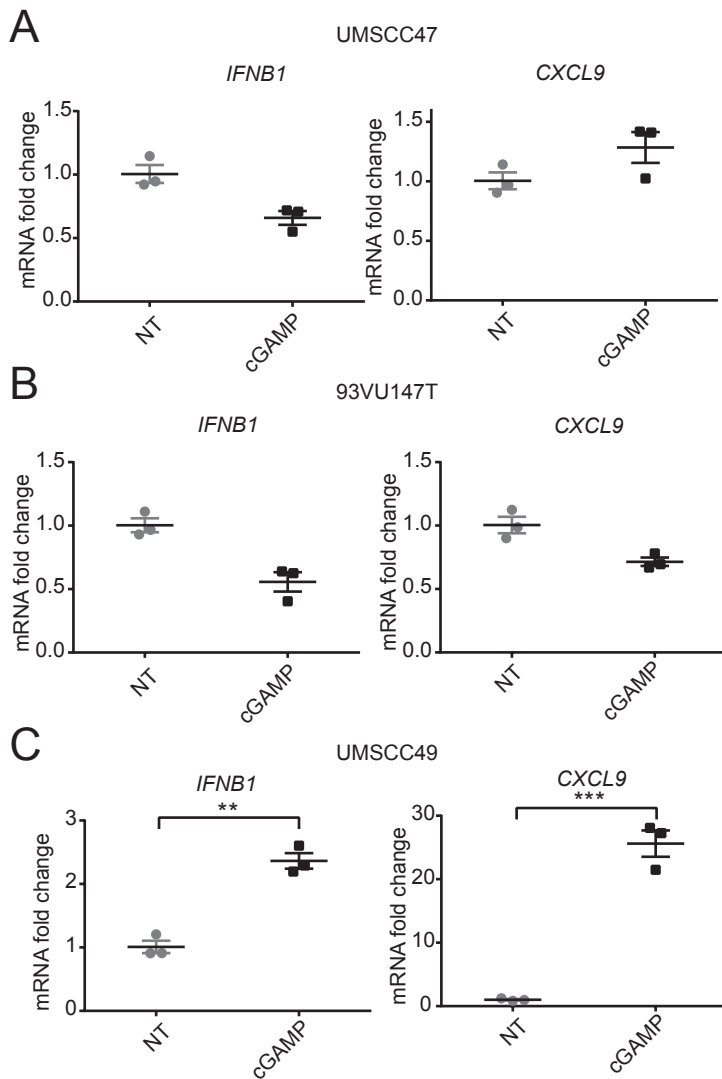
B



Supplemental Figure 2

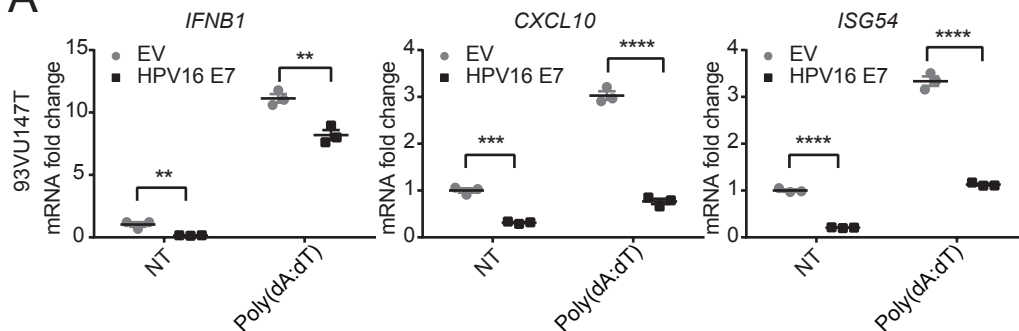
HPV16 E7 1 MHGDPTLHEYMLDLQPET TDLYCYEQLNDSSEEEDEIDG PAGQAEPDRAH 51
HPV18 E7 1 MYGPKATLQDIV LHLEPQNEIPVDLLCHEQLSDSEEEENDEIDGVNHQHL PARRAEPQR 58
HPV16 E7 52 YNIVTF CCKCDSTLRLCVQSTHV DIRTLED LLMG TLGIVCP ICSQKP 98
HPV18 E7 59 HTMLCM CCKCEARIE LVVESSAD LRAFQQLFLS TFSFVCPWCASQQ 105

Supplemental Figure 3

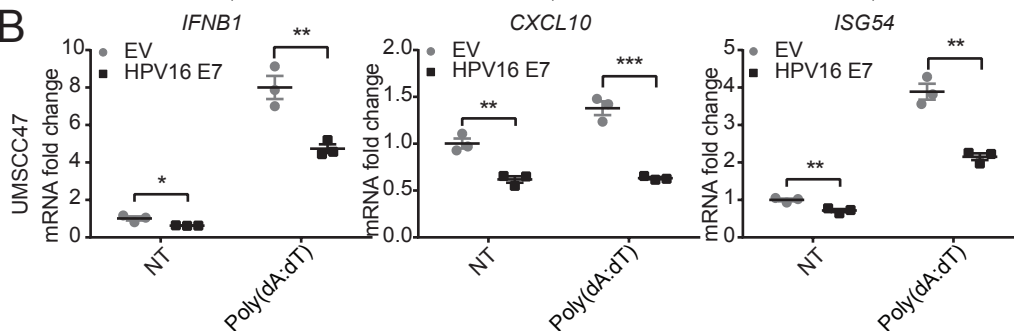


Supplemental Figure 4

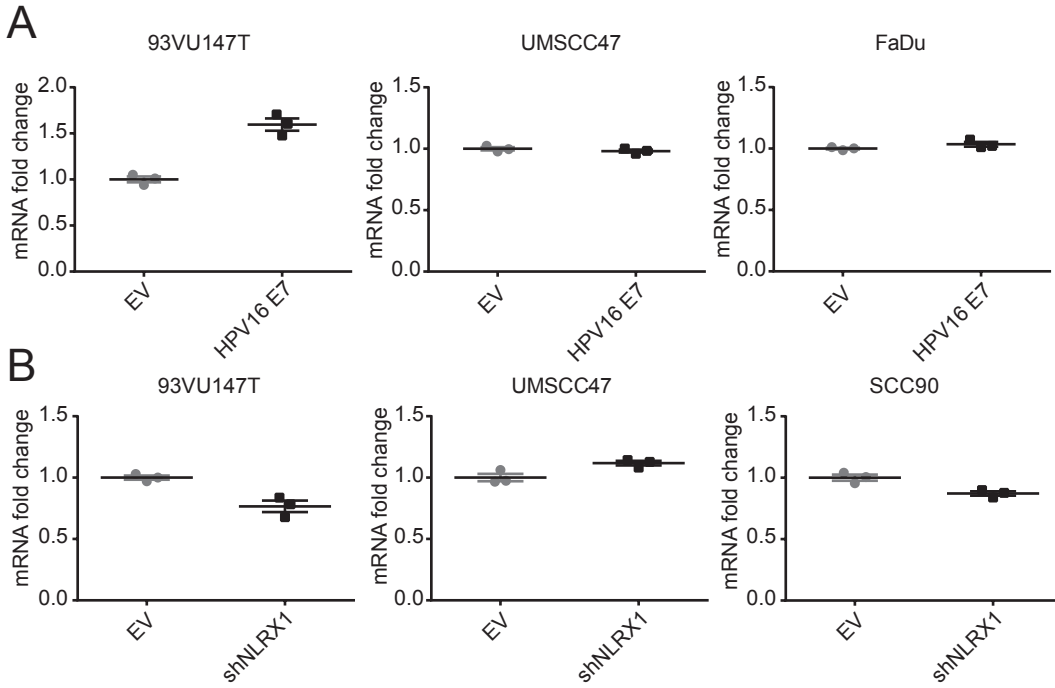
A



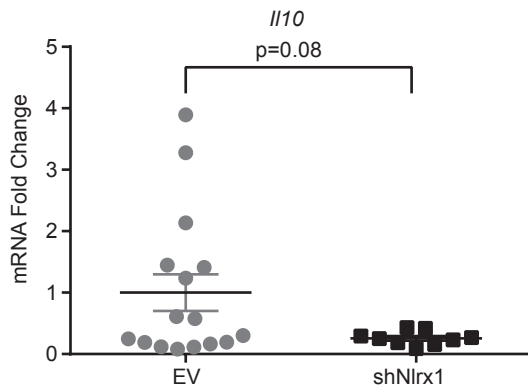
B



Supplemental Figure 5

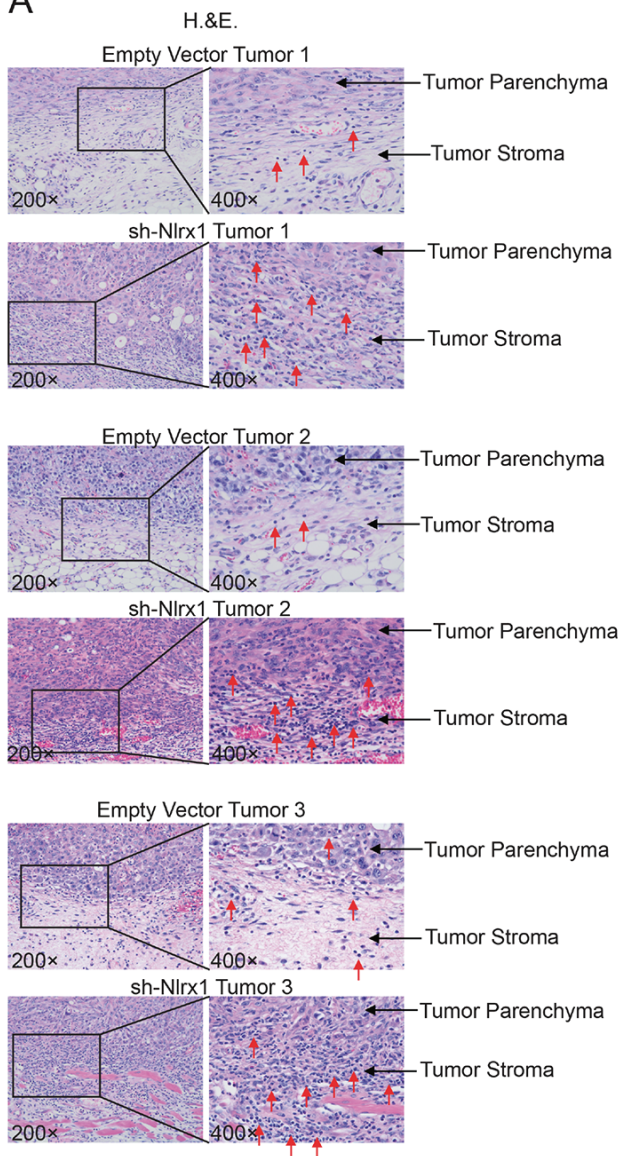


Supplemental Figure 6

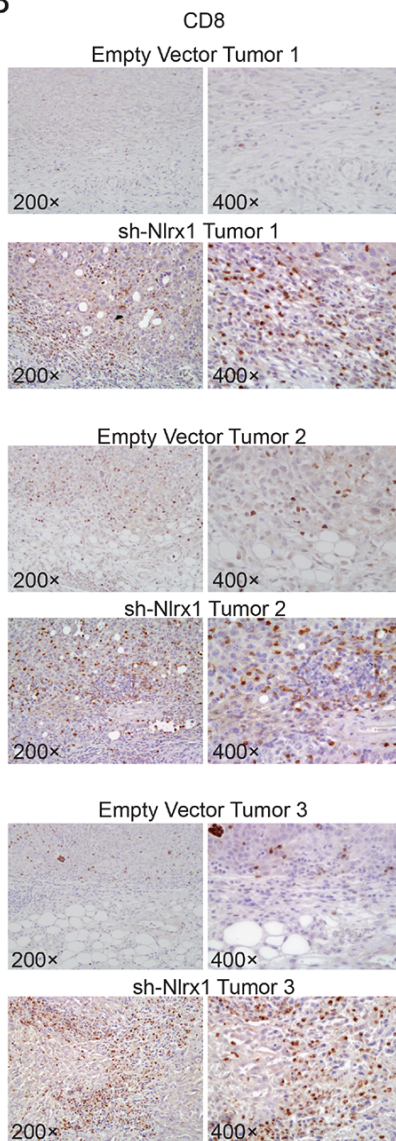


Supplemental Figure 7

A

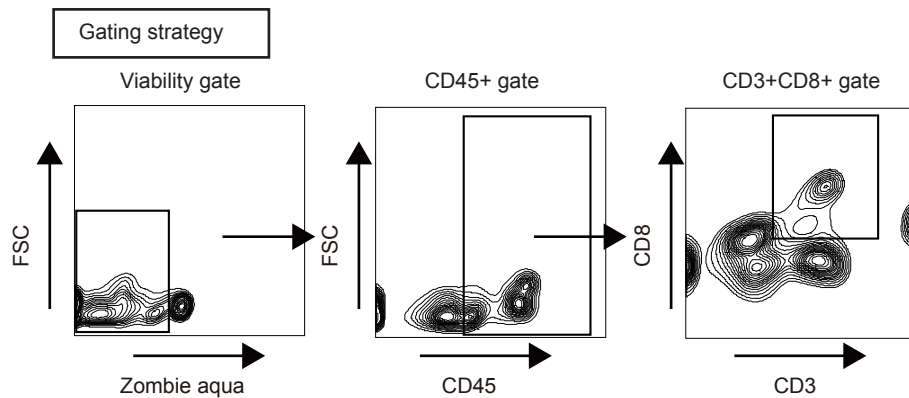


B

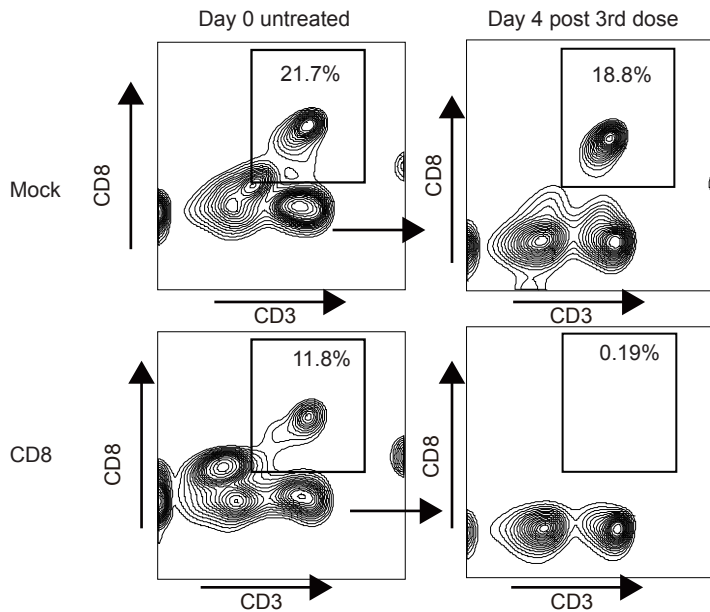


Supplemental Figure 8

A



B



Supplemental Figure 9

